

Structure and Scaling of Polymer Brushes near the Θ Condition

S. Michael Kilbey II*

Department of Chemical Engineering, Clemson University, Clemson, South Carolina 29634

Hiroshi Watanabe

Institute for Chemical Research, Kyoto University, Uji, Kyoto 611-0011, Japan

Matthew Tirrell

Departments of Chemical Engineering and of Materials, Materials Research Laboratory, University of California, Santa Barbara, Santa Barbara, California 93106

Received August 1, 2000; Revised Manuscript Received May 8, 2001

ABSTRACT: We have examined the forces of interaction between opposing polystyrene brushes of various molecular weights in cyclohexane near the Θ temperature. The force–distance profiles and structural information obtained from surface forces experiments are compared to those of brushes in the good solvent, toluene. In both solvents, the chains are stretched a few times their free solution radii of gyration, though we find that when the solvent quality is decreased from good to near- Θ , the brush chains contract more than would free coils in solution undergoing the same solvent change. This shrinkage of the brushes measured from surface forces experiments agrees with hydrodynamic measurements of the layer thickness and theoretical predictions. A mean-field model successfully coalesces the surface forces data of different brushes in the near- Θ solvent to a single universal profile; however, this master curve is distinct from the universal profile formed by brushes bathed in a good solvent. We also show that in near- Θ cyclohexane the osmotic free energy that swells the tethered layer is more than an order of magnitude higher than the corresponding homopolymer solution of the same concentration. Although such a difference was seen for well-solvated brushes, here the magnitude for near- Θ conditions is considerably greater. We assert that the extra repulsion arises because the cyclohexane is a marginal solvent for the tethered chains (similar to the situation for branched chains in solution) and show, by superposing the force–distance data from brushes in both toluene and near- Θ cyclohexane, that $\nu > 0.5$, where ν is the exponent relating the radius of gyration to molecular weight. Additionally, we report the results of experiments using a bimodal brush and discuss how its arms of different length affect its structural behavior.

Introduction

Many applications for polymers require that they adsorb at interfaces or surfaces. The ability to manipulate the structure and properties of the adsorbing layer provides a route to affect the adherence of materials, the rheology of colloidal suspensions, and the lubricative or wear properties of the surface. One particular class of effective surface-modifying agents is A–B diblock copolymers. The amphiphilic nature of these materials allows them to straddle phase boundaries and form “polymer brushes” of moderate density by self-assembly. These interfacial layers can be used to confer desirable properties to the surface.

Polymer brushes can be self-assembled onto a solid surface by using a solvent that is good for one block but poor for the other.^{1–7} This scheme of tethering A–B diblock copolymers to a substrate is often referred to as preferential or selective adsorption. The nonsolvated block adsorbs in a thin layer on a surface, driven by its desire to minimize its contact with the solvent. The adsorption of this “anchor” block tethers the well-solvated “buoy” block to the surface. When the distance between adjacent chains is less than the free-solution radius of gyration of the buoy block, the tethered layer becomes crowded. To alleviate the lateral crowding, the well-solvated blocks stretch away from the surface, resulting in the brush structure depicted by Figure 1.

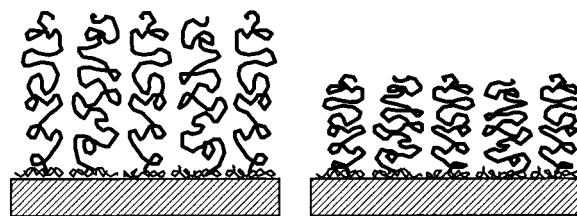


Figure 1. Schematic drawing of a brush in good solvent (left) and less than good solvent (right). The contraction of the brush stems from the less favorable segment–solvent interaction.

Brushes can also be made using triblock copolymers that tether through the center block,⁴ with end-functionalized chains,^{8,9} or by growing polymers from the surface.^{10,11} In each case the underlying physics governing the structure of the constructed brush is the same: the osmotic swelling of the brush layer is balanced by the elastic stretching of the chains. The balance struck between the chains deforming to reduce segment–segment interactions, and the penalty for chain stretching can be described by the fundamental interactions between the segments and the solvent or among segments.^{12–14} The most distinguishing characteristic of brush systems is that the height of the stretched layer, L , is proportional to the number of segments of the brush chain, or $L \sim N$.

To use brushes for the applications listed above, it is important to understand the configurations adopted by the chains, how the layer responds to changes in the solvent environment, and the behavior of the surface

* Corresponding author.

layer due to relative motion of the solvent. One technique that has been widely used to study structure–property relationships of brush systems is the surface forces apparatus (SFA). With this instrument, the forces of interaction between opposing brush layers as a function of the separation distance can be measured on the molecular level.^{1–5,7,9} These force profiles reflect the interaction energy per unit area and, therefore, the structure of layers as they are compressed against each other. The force profiles depend strongly on the molecular weight of the chains and also on the tethering density and segment size of the chains. As shown by Patel et al.,² the force profiles of different brushes in a good solvent can be coalesced onto a unique master curve by using scaling arguments derived from the Alexander–de Gennes models of a single brush.^{12,13} This idea was extended by Watanabe and Tirrell³ when they developed a dimensionless universal profile that quantitatively estimates the coefficients of the model by Patel et al.² This revised predictive model scales the dependence on molecular weight, tethering density, and segment size and readily lends itself to comparison with force profile data from SFA experiments. Adaptations of this model have been successful in describing the structural behavior of multicomponent brushes⁴ and also for opposing brushes of dissimilar materials.³ A model developed by Milner et al.^{14,15} that determines the segment density distribution locally has also been successfully used to predict the force profiles for brushes in good solvents.

Although the Alexander–de Gennes ansatz views the concentration profile of the brush as step-like, with the chains uniformly stretched and their ends localized at the outer edge, in actuality the segment density distribution varies with distance from the tethering surface—the profile of a brush in a moderately good solvent is parabolic with an exponentially decaying tail. This has been confirmed by self-consistent-field calculations,^{14–19} Monte Carlo^{17,20} and molecular dynamics simulations,²¹ and neutron scattering experiments.^{8,22,23} Nevertheless, the simpler Alexander–de Gennes description is useful because it correctly predicts scaling relationships, estimates average properties, and represents a physically accurate picture of a brush when the chains are compressed, since compression eventually results in a nearly steplike segment density profile. Also, as pointed out by Patel and Tirrell, the differences between the forces of interaction predicted for a parabolic and steplike segment density profile are only important at weak compression.⁵ It is these features that lead to the utility of the predictive universal profile model that describes the structural behavior of brushes bathed in a good solvent.

While the structural features of well-solvated brush layers have been thoroughly studied, there are no correspondingly thorough studies of brushes near the Θ condition. Therefore, the goals of the work described in this article were to study the brushes of different molecular weights and tethering densities in a near- Θ solvent and to determine whether the forces of interaction between brushes in this solvent condition can be coalesced by scaling into a universal profile. The results from these two thrusts will be compared to results from brushes in good solvent to form a more complete picture of the structural behavior of brush systems.

Table 1. Size and Adsorption Characteristics of the Block Copolymers Used To Make PS Brushes

polymer	$M_{w, PS}$	dried layer thickness T (Å)	tethering density σ (chains m^{-2})	\bar{P}^* (Å)	$\bar{P}^*/2R_g^a$
(45–55)k	55 000	25.5	1.60×10^{16}	89	0.55
(15–90)k	90 000	32.0	1.87×10^{16}	83	0.38
(70–70)k	70 000	22.0	0.98×10^{16}	114	0.60
(39–102–62)k	50 500 ^b	18.0	1.11×10^{16}	107	0.69 ^b

^a A value of $\bar{P}^*/2R_g < 1$ indicates that the chains were crowded and brushes were formed. ^b Based on the equivalent diblock.

Materials and Methods

The block copolymers made from polystyrene (PS) and poly(vinylpyridine) (PVP) that were studied in this work are listed in Table 1. Throughout this article we will refer to the diblock copolymers, for example, as (45–55)k PVP–PS, where the numbers refer to the molecular weight, in thousands, of the PVP and PS blocks, respectively. A single (38–102–62)k PS–PVP–PS triblock copolymer was also studied. These materials were anionically polymerized, the details of which have been previously published.³ The protocols for making polymer brushes from both diblock and triblock block copolymers in the SFA have been well documented,^{1–5} so only a few points of the procedure are presented here.

Brushes were self-assembled on the opposing mica surfaces of the SFA from toluene solutions that contained the block copolymer at a submicellar concentration—the diblocks at <30 mg/L and the triblock at <10 mg/L. It is important to do the adsorption in toluene, even for eventual work in cyclohexane, to prevent the PS blocks from adsorbing directly on the mica. In toluene the PVP block strongly adsorbs on the surface, tethering the PS block(s) to the substrate by their ends. At least 8 h was allowed for this self-assembly process to occur, and as with previous experiments,^{1–4,25} the temperature was held at 32 ± 0.1 °C throughout the experiment. Following preferential adsorption of the brushes, force profiles in toluene were recorded, and then the solvent was changed to cyclohexane. Cyclohexane also is a poor solvent for PVP, but at 32 °C it is a near- Θ solvent for the PS brushes. (The Θ temperature for untethered PS chains in cyclohexane is 34.5 °C, whereas the critical point for PS of molecular weight 55 000 g mol^{-1} is ~ 16 °C.²⁴) The force profiles for the PS brushes in cyclohexane were recorded, and then the solvent was replaced with toluene. This step allowed us to reexamine the force profiles in the good solvent to determine whether there were structural changes since the brush was first constructed. Toluene (EM Scientific, HPLC grade) was used as received, but the cyclohexane (Fisher, HPLC grade) was distilled to remove trace amounts of water. All solvents were also filtered through a 0.22 μm filter (Millipore) prior to use. After gathering all force data, including friction measurements reported elsewhere,²⁵ the brushes were dried so that the surface density of chains could be determined from the thickness of the dried layer. This procedure has been described elsewhere as well.^{3,4}

From the surface density of chains, an average distance between the tethering points of adjacent brush chains, \bar{P}^* , can be calculated using the assumption that each chain occupies a cylindrical volume whose base is coincident with the tethering surface. Brushes form when this distance is less than twice the free solution radius of gyration of the nonadsorbed block (in our case, the PS block), or $\bar{P}^*/2R_g < 1$. The values of $\bar{P}^*/2R_g$ calculated in Table 1 are based on the R_g in toluene. For the case of a brush formed from an A–B–A triblock copolymer, it is useful to evaluate its structure in terms of the “equivalent” A–B diblock copolymer. As explained by Dhoot et al.,⁴ averaging the molecular weight of the two A arms and halving the size of the B anchor block of the triblock copolymer yields the equivalent diblock copolymer. This transformation, which is useful for scaling studies discussed below, preserves the tethering density of the layer and represents the number of brush segments by the average of the two arms. The adsorption characteristics of the brush layers, specifically the dry layer thickness, surface density of chains, σ , and $\bar{P}^*/2R_g$, are

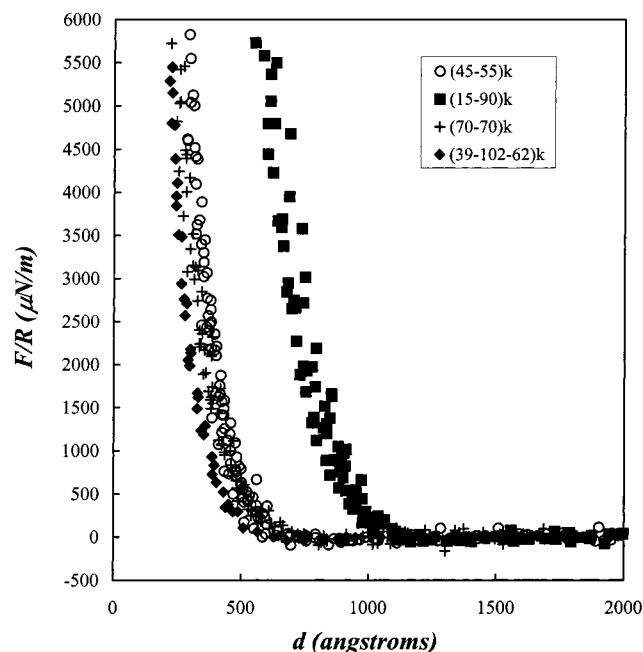


Figure 2. Normal force profiles for PVP-PS diblock copolymers and a PS-PVP-PS triblock copolymer in toluene at 32 °C. The layers resist compression against one another, and the range at which the forces of interaction are detected indicates that the PS brushes are stretched a few times their free solution radii of gyration.

presented in Table 1. R_g values were calculated from correlations based on the light scattering and viscosity experiments reported in refs 26–28.

Results and Discussion

Force Profiles and Chain Stretching. The force profiles for the brushes in toluene and cyclohexane are shown in Figures 2 and 3, respectively. They are presented as the force of interaction normalized by the radius of curvature of the brush-bearing surface, F/R , which is directly proportional to the interaction energy per unit area,²⁹ vs the surface separation distance. (Throughout this text, we use the term force and F/R interchangeably when discussing SFA results.) In each of these solvents the forces between the brush bearing surfaces are monotonically repulsive; the strong repulsion arises from the fact that as the two brushes are forced together, the average segment concentration between the surfaces increases, thus increasing the osmotic pressure (or force) that resists further compression. Even though the measurements in cyclohexane are made at a temperature slightly below the Θ temperature for untethered PS chains, we see no attractive interactions in the force profiles—the dispersive effect remains stable. The ranges at which repulsion is seen, as well as the data in Table 1, indicate that all of these block copolymers formed brushes. Since there is a brush on each surface, one-half of the distance at which repulsive normal forces are detected is used as a measure of the height of the brush. It is clear that in both solvents the brushes are stretched a few times the free solution radius of gyration of the PS chains. This is quantified in Table 2, which compares the brush heights as determined from SFA experiments to the R_g of a PS coil that has the same molecular weight as the buoy block of the brush.

It is worth noting that for the brushes made from the diblock copolymers, as the lateral crowding increases

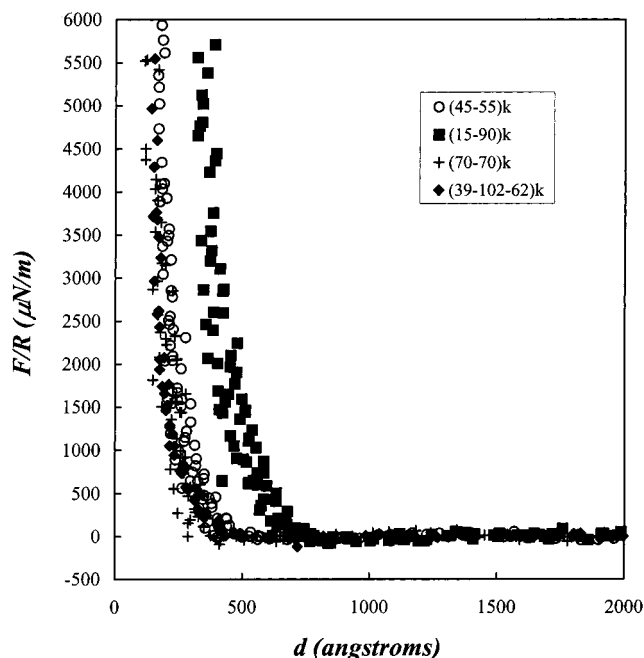


Figure 3. Normal force profiles in cyclohexane at 32 °C for PVP-PS diblocks and a PS-PVP-PS triblock copolymer. The forces of interaction between the PS brushes are repulsive, and the distance at which forces become nonzero indicates that the brushes are stretched a few times their free solution radii of gyration.

Table 2. Comparison of the Size of PS Tethered Chains Relative to Their Size as Coils in Free Solution

polymer	toluene			cyclohexane		
	R_g^a (Å)	L (Å)	L/R_g	R_g^a (Å)	L (Å)	L/R_g
(45–55)k	81	310	3.83	70	205	2.93
(15–90)k	110	545	4.96	89	355	3.99
(70–70)k	95	338	3.56	79	188	2.38
(39–102–62)k	78 ^b	275	3.53	67 ^b	218	3.25

^a Calculated from viscosity and light scattering measurements reported in refs 26–28. ^b R_g of the triblock copolymer is based on the equivalent diblock.

(decreasing I^*/R_g), the degree to which the chains are stretched relative to their R_g increases. This is observed in both toluene and near- Θ cyclohexane. The triblock copolymer does not fit in this trend because the molecular weight used to calculate R_g of the triblock was based on a simple average of the two PS arms. This is not the correct molecular weight for characterizing the total extension of the brush, which is what is sensed by the SFA when two opposing brushes contact one another. The long and short PS arms of a bimodal brush stretch to different degrees, leading to a complex segment density distribution that depends on the relative size and amounts of the long and short chains, ultimately controlling the brush height.³⁰ Also, using the average PS molecular weight to establish the threshold for lateral crowding on the surface is simplistic because it ignores the influence the center PVP block has on the spacing between the two PS arms. We will revisit the issue of how to treat the triblock copolymer later in this paper. Nevertheless, while these brushes made from diblocks are stretched a few times their R_g , it has been shown that end-anchoring a chain to a surface through a chemical bond produces brushes that are stretched up to 10 times their R_g ,⁸ and growing a brush chain through a living polymerization from a surface can produce brushes that are even more strongly stretched.^{10,11}

Table 3. Calculated and Experimentally Measured Ratios of the Sizes of Coils and Brushes in Different Solvents (Tol = Toluene, CH = Cyclohexane)

polymer	$R_{g,Tol}/R_{g,CH}^a$	$(L_{Tol}/L_{CH})_{exp}^b$	$(L_{Tol}/L_{CH})_{theo}^c$	$(L_{Tol}/L_{CH})_{theo}^d$
(45–55)k	1.16	1.51	1.47	1.54
(15–90)k	1.24	1.54	1.49	1.50
(70–70)k	1.20	1.80	1.55	1.67
(39–102–62)k	1.16 ^e	1.26		

^a Calculated from viscosity and light scattering measurements reported in refs 26–28. ^b Measured from SFA experiments. ^c Based on scaling treatment described in ref 33. ^d Based on explicit expression for brush height described in the Appendix and ref 31. ^e R_g of the triblock copolymer is based on the equivalent diblock.

In addition to comparing the brush heights to the size of solvated coils in the same solvent conditions, we can use the SFA data to quantify the contraction of the brushes when the solvent condition is changed from the good solvent (toluene at 32 °C) to the near- Θ solvent (cyclohexane at 32 °C). This contraction can be compared with the shrinkage in the R_g of PS coils in free solution of the same molecular weight. We express the contraction by the ratio of the spatial extent of the PS chain in the good solvent to that in the Θ solvent, and these data are presented in Table 3. From these data, it is apparent that brushes undergo a more pronounced reduction in size than the free coils when the solvent condition worsens.

The data also show that the brush made from the (70–70)k PVP–PS shrinks more than the other two diblock brushes when the solvent is changed. This is due to the effect of tethering density on brush structure: more densely grafted brushes contract less because the lateral crowding between chains prevents the chains from contracting. The more significant contraction of the brush made from the (70–70)k PVP–PS, which has the lowest tethering density of the three diblock brushes, is predicted by the analysis developed in ref 31 and summarized in the Appendix. (Theoretical analyses of the extent of brush contraction that occurs when the solvent is changed are fully discussed below.) There may also be an effect of lateral rearrangement of the chains on the surface that is known to occur when the solvent is changed from good to Θ . This reorganization has been observed in AFM studies by Kelley et al.³² The surface rearrangement of the less dense brush may provide an additional avenue for the chains to reorganize and diminish their contact with the near- Θ cyclohexane by increasing the volume available for the chain contraction. We do not believe that chain desorption, which will be addressed later in this article, was a factor here.

The extent to which the brushes made from the diblocks contract when the solvent is changed can be compared against other theoretical and experimental studies. Halperin formulated scaling expressions for the solvated height of end-tethered chains in good, Θ , and poor solvents based on two contributions to the total free energy of the layer—an entropic contribution due to coil deformation and a free energy of mixing derived from a virial expansion.³³ For a good solvent, $L_g \sim m^{1/3} N \sigma^{1/3} b^5/3$, and for a Θ solvent, $L_\theta \sim n^{1/4} N \sigma^{1/2} b^2$, where, as described in ref 33, m and n are related to the second and third virial coefficients, respectively, and b is the segment size. Values for the second and third virial coefficients for PS in toluene²⁷ and cyclohexane²⁸ along with the

tethering densities and molecular weights of the PS brush chains were used to predict³³ $L_{toluene}/L_{cyclohexane} = 1.50 \pm 0.05$, which is similar to our results despite the fact that the scaling treatment omits numeric prefactors.

Numeric prefactors are included in the explicit expression for brush height developed in ref 31 (and briefly summarized in the Appendix), and this can also be used to quantify the height change associated with the solvent switch. Equation A10 results from considering the osmotic and elastic contributions to the free energy of a brush and using a correlation length based on an isolated, uncompressed brush without lateral heterogeneity, rather than coils in free solution.³¹ Coupling the analysis presented in the Appendix with experimental data (e.g., tethering density and degree of polymerization of the brush chains) leads to the results shown in the rightmost column of Table 3; the calculated ratios of the equilibrium brush height in toluene to that in cyclohexane range from 1.50 to 1.67 for the diblocks studied, and the less densely grafted brush made from the (70–70)k PVP–PS undergoes a significantly greater contraction. These conclusions mirror the SFA measurements.

Webber et al. investigated⁶ how the hydrodynamic thickness of preferentially assembled diblock copolymer layers in capillary pores depends on the solvent quality. The hydrodynamic thickness of a surface-modifying layer was calculated on the basis of the flow of solvent through a membrane. They obtained results for three PVP–PS diblock systems: an (8–46)k, (3–57)k, and (3–80)k were studied in toluene at 25 °C and cyclohexane at T_θ , and the degree of contraction ($L_{toluene}/L_{cyclohexane}$) was found to be 2.23, 1.42, and 1.62, respectively. Although no data on the tethering density of these layers were reported, based on their procedure for self-assembly of the layer and the calculated hydrodynamic layer heights, we suspect the adsorbed amounts were not significantly different from those in our SFA experiments. Using a series of PVP–PS diblock copolymers that were preferentially adsorbed from toluene, Parsonage and co-workers³⁴ showed that although the surface density of chains may vary slightly, the mass coverage of these polymer amphiphiles remains about the same.

The data in Table 3 also indicate that the contraction of the brush made from the triblock copolymer is smaller than that seen for diblocks and in fact closely parallels the contraction of free coils in solution. This can be explained in terms of the bimodal structure of this brush; there is an inner stratum comprised of the short arms and a portion of the long arms and an outer stratum composed of the part of the long arms that extend above the inner strata. As shown by Dhoot et al.⁴ in an independent study, the outer stratum of a surface-tethered layer made from this triblock copolymer is not dense enough to actually form a brush. Essentially, the structure of this “brush” is that of a brush covered with a diffuse layer that has a structure resembling coils. When the solvent condition is changed from a good solvent to a near- Θ solvent, there is a contraction of both strata—the inner brush and outer coils—and this is what is sensed by the SFA experiment when the two opposing layers are brought into contact. Coils do not shrink as much as brushes do; thus, the overall shrinkage of the bimodal brush is probably a composite of the contraction of the chains that form the

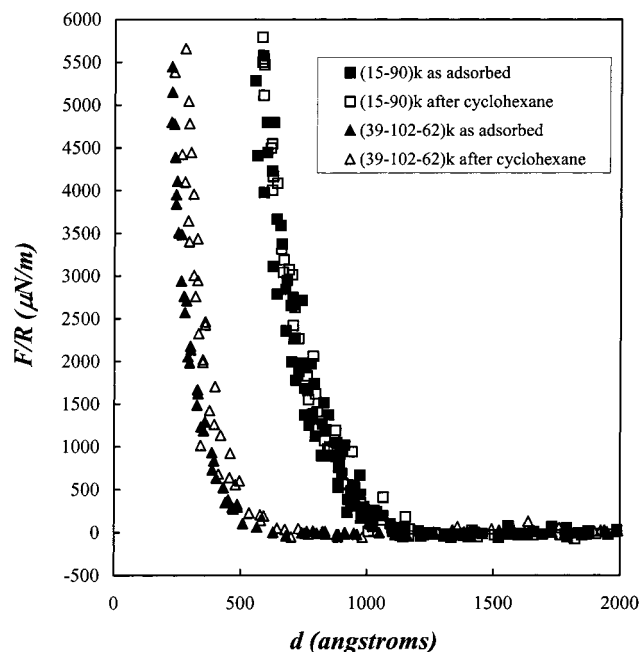


Figure 4. Normal force profiles for a PVP-PS diblock copolymer and a PS-PVP-PS triblock copolymer in toluene at 32 °C. The profiles labeled “as adsorbed” were recorded after adsorption of the polymer brush. The profiles labeled “after cyclohexane” were recorded after the solvent was changed back to toluene after experiments in cyclohexane were completed. The agreement between the pair of profiles indicates that there is essentially no chain desorption.

inner layer brush and a minor amount of shrinkage of the coil-like, diffuse outer layer.

Following the experiments in cyclohexane, the solvent was changed back to toluene, and the normal forces were again measured. Figure 4 shows force data for one of the diblock brushes and the triblock brush. The data for the other diblock brushes are omitted for clarity, but the results are analogous. Within experimental error, the profiles following the solvent changes coincide with the initial toluene force profiles. This indicates that the structural behavior of the brush “as adsorbed” and following the solvent changes to and from cyclohexane is the same, and the poorly solvated PVP fulfills its role of anchoring the brush to the mica substrates. On the basis of these results, we do not believe that chain desorption is significant in these experiments. This is an intriguing result given the AFM studies showing rearrangement of the chains on the surface when the solvent is changed from toluene to cyclohexane.³² Since the force profiles are intimately connected to the structure of the brush layer, the force profiles in Figure 4 suggest that the layer structure reverts back to its initial structure when the solvent is changed back to toluene.

Evidence for Universal Behavior. With the normal force profiles and surface density of chains determined experimentally, the osmotic contribution to the free energy of the brush can be examined and compared to that of homopolymer solutions. For highly compressed brushes in a good solvent, chain stretching and the resultant elastic forces are eliminated, the osmotic forces are a function of concentration only, and they dominate the behavior of the layer. Since the forces of interaction become independent of molecular weight and tethering density in this limit, a predictive universal profile can be developed to describe the structure of brushes. This

has been done for brushes immersed in a good solvent,³ and here we seek to do the same for brushes in the near- Θ solvent.

To make a comparison between the osmotic pressure behavior of the tethered chains and bulk homopolymer solutions, it is useful to recast the SFA data in terms of segment concentration instead of separation distance. The average concentration of segments between the surfaces can be calculated from the surface density of chains: $c = 2\sigma M_{PS}/N_{Av}(d - 2L_{PVP})$. This expression is simply the mass of chains per unit area divided by the distance between the brush surfaces. The reduction of the separation distance, d , by $2L_{PVP}$ is a minor correction that eliminates the thickness contribution of the adsorbing block present on each of the opposing brushes in the SFA. L_{PVP} is calculated by multiplying the dried layer thickness by the ratio of the molecular weight of the anchor block to the molecular weight of the copolymer. Basing the thickness of the PVP layer on the dry layer thickness ignores any swelling of this block; this assumption should be fairly good since PVP is poorly solvated by the solvents used in the experiments.

An equation for the reduced osmotic free energy of the brush layer in a form adapted for use with SFA data is given by Watanabe and Tirrell:³

$$\Delta f_{os,b} = [(m_0/N_{Av})^{3\nu/3\nu-1}/(wkT(4\pi b^3/3)^{1/3\nu-1})](F/2\pi R) \quad (1)$$

In this equation, m_0 is the mass of the monomer, b is the segment size, and w is the mass of chains per unit area, $2\sigma M_{PS}/N_{Av}$. The factor of 2π dividing F/R in this equation stems from the Derjaguin approximation²⁹ and converts the force data to energy per unit area.³ ν is the exponent that scales R_g as a function of N ; $R_g = bN^\nu$. For PS in cyclohexane at T_θ , $\nu = 0.5$ and $b = 3.047$ Å.³⁵

The osmotic contribution to the free energy of the layer according to eq 1 is plotted as a function of concentration in Figure 5. When the brushes are strongly compressed (high c or low d), we see evidence that the curves are merging, indicating that the osmotic forces that swell the layer are indeed becoming independent of molecular weight and tethering density. The level of compression that must be achieved in order to see the profiles converge is quite high. At these levels, the osmotic interaction dominates the force profiles. At low levels of compression where the brushes first come into contact, differences in the entropic elasticity resisting stretching of the chains, which depends on the tethering density and molecular weight, give rise to the distinct profile for each brush.

Since the coils of the brushes are overlapped but not highly concentrated, it is appropriate to compare the SFA data with the osmotic pressure as a function of concentration for a polystyrene homopolymer solution in the semidilute regime. The osmotic free energy of a homopolymer solution, $\Delta f_{os,s}$, reduced to the same basis as eq 1 is given as³

$$\Delta f_{os,s} = -[(m/N_{Av})^{3\nu/3\nu-1}/(wkT(4\pi b^3/3)^{1/3\nu-1})] \int_{x=\infty}^{x=d} \pi[c(x)] dx \quad (2)$$

As explained by Watanabe and Tirrell, the purpose of the integral is to calculate work (per unit area) done against osmotic pressure to concentrate a solution from infinite separation down to a given surface separation.³

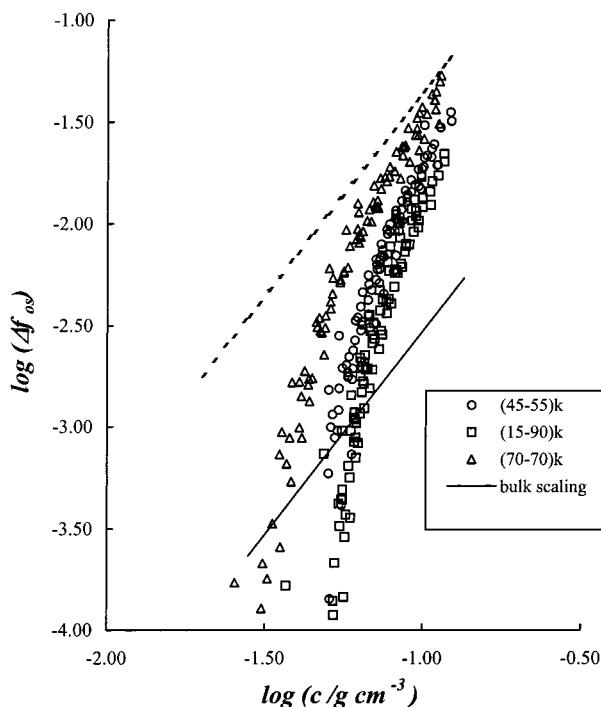


Figure 5. Comparison of the osmotic forces of interaction for diblock brushes and a PS homopolymer solution (solid line). The osmotic free energy of the brush (cf. eq 1) quickly exceeds that of the homopolymer solution (cf. eq 4) when the layers are pressed together. At low levels of compression, differences in the stretching energies of each brush produce a distinct curve, but at high levels of compression, the curves for each brush merge because the osmotic pressure depends only on the average concentration of segments between the surfaces. The dashed line, which has the same slope as the solid line representing bulk behavior, is a guide to the eye showing that, in the limit of strong compression, the concentration dependence of the brush layers is the same as the bulk solution.

Inserting a power-law model for the osmotic pressure of homopolymer solutions in the semidilute regime,^{36,37}

$$\pi M/cRT = K_{\pi}(c/c^*)^{1/3\nu-1} \quad (3)$$

and carrying out the integration of eq 2, yields the result

$$\Delta f_{os,s} = (3\nu - 1)K_{\pi}c^{1/3\nu-1} \quad (4)$$

Thus, to compare the osmotic free energy of the brushes to homopolymer solutions of the same concentration, only K_{π} and ν must be determined.

Unfortunately, tabulated data of the osmotic pressure of PS in cyclohexane in the semidilute regime at the Θ condition are scarce and do not cover a large enough range of reduced concentration (c/c^*) to obtain a concrete value of K_{π} . (A value of $K_{\pi} = 2.2$ for PS in toluene is available from the extensive work of Noda et al.³⁸) Part of the problem is that to be in the semidilute regime in a Θ solvent, high molecular weights are needed to have both a large value of c/c^* but low values of c . An estimate for K_{π} can be obtained from the results of Stepanek et al.³⁹ Their empirical expression for the osmotic compressibility ($\partial\pi/\partial c$) as a function of concentration for semidilute solutions of PS in cyclohexane at $T = T_{\theta}$ can be equated to the derivative (with respect to c) of eq 3. When the numerical and material constants are inserted, we calculate $K_{\pi} = 2/3$ with the only assumption being made is that K_{π} does not depend on concentration over the range they examined.

The osmotic free energy of a PS homopolymer solution plotted according to eq 4 using $\nu = 0.5$ and $K_{\pi} = 2/3$ is depicted by the solid line in Figure 5. The curves for the brushes cross this line at relatively low concentrations, indicating that slight compression of the brushes results in their osmotic free energy exceeding that of the homopolymer solution. The dashed line in Figure 5 that lies above the data has the same slope as the bulk scaling and appears to be roughly asymptotically tangential to the data, which shows that when strongly squeezed, the characteristic response of the brushes is similar to the bulk solution. The fact that the concentration dependencies of the osmotic free energy of the highly compressed brushes and homopolymer solution are the same is not surprising; in each case, only the average concentrations of segments in the system are expected to be important. However, the osmotic free energy of tethered brushes at high compression (dashed line) is greater than the osmotic free energy of untethered chains (solid line) by a factor of ~ 15 . An analogous discrepancy between the osmotic free energy of tethered chains and coils in free solution was also seen for PS in toluene; however, the difference between these was a factor of about 2.³

Recently, this difference between the osmotic free energy of brushes and semidilute solutions of untethered chains was analyzed³¹ and found to be due to the erroneous assumption that the correlation lengths of tethered and untethered chains were the same. As briefly summarized in the Appendix, if the proper correlation lengths are used to derive the osmotic free energy of the brush (cf. eq 1) and untethered system (cf. eq 4), then the scaling analysis yields $f_{os,b}(c)/f_{os,s}(c) \cong 2.2$ for PS chains in good solvents and $f_{os,b}(c)/f_{os,s}(c) \cong 3.4$ for PS chains in Θ solvents. While this explains the difference between the osmotic free energy of brushes and free coils in toluene,^{3,31} it cannot explain the factor of 15 seen in Figure 5 for brushes in near- Θ cyclohexane.

We propose that this difference might be attributed to an extra monomer–monomer repulsion arising from the tethered structure. In other words, cyclohexane at 32 °C seems to be a marginal solvent for the tethered PS chains. A reduction in T_{θ} is known to occur for branched polymers, i.e., star and comb polymers. For example, as the number of branches on a polyisoprene star increases from 3 to 22, T_{θ} in methyl propyl ketone decreases from 33 to 23.5 °C, and T_{θ} of a comb PS polymer in cyclohexane decreases from 36 to 20 °C.⁴⁰ The extra monomer–monomer repulsion due to branching is not important in good solvents where the repulsion is sufficiently strong, even in the absence of branching. However, the extra repulsion for branched chains in Θ solvents considerably affects the thermodynamic properties. We will revisit and buttress our assertion later in this paper.

Scaling of the Force Profile Data. Figure 5 shows that if only the osmotic contribution to the free energy of the brushes immersed in the near- Θ solvent is considered, the profiles merge in the limit of strong compression. If the entropic penalty for chain stretching were also taken into account, we would expect that the force profiles from SFA experiments would coalesce to a single master curve. This was demonstrated by Watanabe and Tirrell for polystyrene and polyisoprene brushes in toluene³ and by Dhoot et al.⁴ for multicomponent brushes made with chains of different lengths.

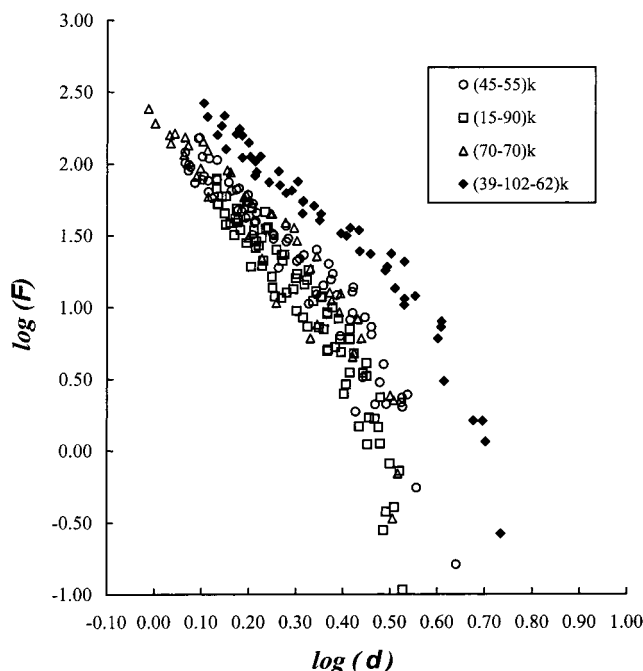


Figure 6. Master curve for brushes bathed in the near- Θ cyclohexane. The scaled force profiles for the brushes formed from diblock copolymers coalesce to a single curve, particularly at mid to high levels of compression. Only at high compression where the osmotic interaction dominates the free energy of the layer does the scaled force profile of the triblock copolymer (filled symbols) approach the curve suggested by the diblocks (open symbols).

In those studies scaling variables derived from the mean-field Alexander–de Gennes model were used:

$$d = (d - 2L_{\text{PVP}})/2Nb^{1/\nu}\sigma^{(1-\nu)/2\nu} \quad (5)$$

and

$$F = (F/R)/(kTb^{1/\nu})N\sigma^{(2\nu+1)/2\nu} \quad (6)$$

In eq 5 the separation distance is again corrected to remove the contribution of the thin PVP layer and normalized by the scaling for the equilibrium brush height. (The factors of 2 arise because there is a brush on each surface.) As before, N and σ are defined as the degree of polymerization of the solvated chain and the tethering density of adsorbed chains, respectively.

Essentially, the dimensionless scaling variable d reduces the measured surface separation distance between the two brush-bearing surfaces by twice the equilibrium height of the uncompressed brush. The dimensionless reduced force, F , scales F/R (again, proportional to the interaction energy of interaction per unit area) by the free energy per unit area of an uncompressed brush. To create the scaled profiles for the brushes studied in this work (Figures 6 and 7), we use the following values for the monomer size and exponent ν : For PS in toluene, $b = 1.86 \text{ \AA}$ and $\nu = 0.595$;⁴¹ for PS in cyclohexane, $b = 3.047 \text{ \AA}$ and $\nu = 0.5$.³⁵

Figure 6, which displays the reduced data for the brushes in cyclohexane at 32 °C, shows that the force profiles for brushes made from the diblock copolymers coalesce to a single master curve, as indicated by the unfilled symbols in the figure. The individual profiles converge at high compression, where the strong confine-

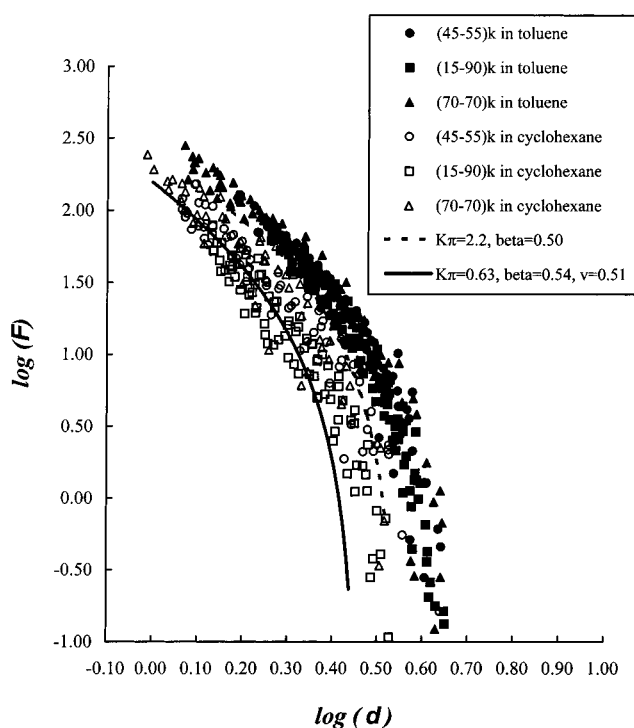


Figure 7. Universal curves for brushes formed from PVP–PS diblocks in toluene and cyclohexane with PTH fits. The force–distance data are scaled according to eqs 5 and 6, and the curves for the brushes in the two different solvents are distinct because of differences in solvent quality and statistical segment size. The PTH fits (dashed and solid lines) are obtained from eq 7. The curve through the cyclohexane data (solid line) formed by the PTH profile with $\nu = 0.51$, $K_\pi = 0.63$, and $\beta = 0.54$ agrees with the experimentally obtained scaled force profiles.

ment overcomes differences in elastic stretching and the osmotic contribution dominates brush behavior. Including the entropic contribution to the free energy of the brush in the model used to derive the scaling variables (eqs 5 and 6) has helped gather the curves from the different diblock copolymer brushes at low levels of compression.

Figure 6 also shows that the force–distance data for the brush made from the triblock (filled symbols) does not coalesce to the curves suggested by the monodisperse diblocks, although it appears that the curves may be tending toward the same limit at high compression. The location of the scaled force curve for triblock, relative to those for the diblocks, is a result of the way that the force–distance data were scaled. By using an N based on the average molecular weight of the PS arms of the triblock, we are underestimating the equilibrium height of the layer. In one sense the scaled data are saying that we detect interactions at a distance exceeding the range at which repulsion would be seen for opposing monodisperse brushes made with arms of the size N that are tethered at the same surface density. As noted by Dan and Tirrell,³⁰ the equilibrium thickness of a bimodal brush is not proportional to the average chain molecular weight; the brush height is also a product of the difference between the size of the arms and the ratio of long-to-short arms. The problem with using the average molecular weight in scaling F/R is more complex. At low compression the mean-field picture of a brush is inappropriate because the brush is not uniformly dense, nor is the periphery strongly stretched. These factors are exacerbated by the bimodal

distribution of chains in the triblock copolymer brush. Thus, in this limit, scaling the force data by the interaction energy of the uncompressed brush based on a mean-field assumption is a poor choice. However, when the layer is sufficiently compressed the osmotic contribution dominates (over the elastic stretching) the free energy of the layer, the mean-field picture of the brush is restored. The mean-field description of the osmotic force that swells the layer depends only on the average segment density of the layer, so in this limit the use of the average molecular weight of the two arms is appropriate. Indeed, at high compression the scaled data for the triblock brush approach that for the brushes made with a single length arm. Ultimately, as was the case for well-solvated bimodal brushes,⁴ these scaling issues cannot be mutually resolved with a mean-field approach, and as a result, the SFA data for bimodal brushes cannot be coalesced to the universal curve in either solvent.

In Figure 7 the reduced force–distance data for the two different solvent qualities studied are plotted in order to understand the relationship between the sets of data produced from diblock copolymer brushes of different molecular weights and tethering densities. Here we see that the data coalesce to form a single profile for each solvent condition. The master curve formed by the brushes in the near- Θ solvent is situated inside the master curve for the brushes immersed in the good solvent. This can be interpreted from two viewpoints: at a given (reduced) distance, the (reduced) forces of interaction between the brushes bathed in the near- Θ solvent are less than those of brushes in a good solvent, or, at a given level of force, the well-solvated brush is swollen to a greater extent than the brush in the near- Θ solvent. Both of these interpretations are also reflected in the unscaled data presented in Figures 2 and 3.

We suspect that the master curve for brushes bathed in the near- Θ cyclohexane is broader than that in toluene due to the surface heterogeneity. Although all brush systems were self-assembled under similar conditions, the reorganization of the chains that occurs when the solvent is changed from toluene to cyclohexane causes local conformation and concentration differences across the surface.³² Since the interactions between the layer are intimately related to the structure, reproducing experimental results and making measurements at different contact spots on a particular set of surfaces results in greater variations between the force profiles.

Predicting the Scaled Force Profiles and Scaling the Dependence on Solvent Quality. For a given solvent condition, the fact that a single curve results from scaling the force–distance profiles suggests that the universal profile could be predicted if the Alexander–de Gennes model can be recast in a form properly scaled for molecular weight and surface density. This has been proven for PS brushes in toluene but not for chains bathed in a near- Θ solvent. To do so would provide another means of testing universal behavior and demonstrate the robustness of the model.

Watanabe and Tirrell derived³ an expression for the universal, dimensionless force–distance profiles for brushes based on osmotic swelling and elastic stretching of the chain. This mean-field model (referred to as the PTH model) relies on three parameters— K_π , ν , and β :

$$F = X\{[Yd^{1/(3\nu-1)} - 1] + (4\nu - 1)^{-1}[Zd^{(4\nu-1)/(3\nu-1)} - 1]\} \quad (7)$$

$$X = 4\pi[(4\nu - 1)/4]^{1/4\nu}[(3\nu - 1)K_\pi]^{(4\nu-1)/4\nu}(4\pi/3\beta)^{1/2\nu} \quad (8)$$

$$Y = \{[4(3\nu - 1)K_\pi]/[(4\nu - 1)]\}^{1/4\nu}(4\pi/3\beta)^{(1-\nu)/2\nu(3\nu-1)} \quad (9)$$

$$Z = \{[4(3\nu - 1)K_\pi]/[(4\nu - 1)]\}^{-(4\nu-1)/4\nu}(4\pi/3\beta)^{-(1-\nu)(4\nu-1)/2\nu(3\nu-1)} \quad (10)$$

The two terms on the right-hand side of eq 7 represent the osmotic and elastic contributions, respectively. As shown previously³ and in Figure 7, the reduced force–distance data for PS in toluene can be adequately fit using $K_\pi = 2.2$ and $\nu = 0.595$, which come from independent experiments on bulk systems,^{38,41} and $\beta = 0.5$. The parameter β corrects for the differences between the osmotic free energy of tethered chains and free coils, and its value is close to the value (0.54) calculated from the analysis presented in the Appendix.

Because we are dealing with tethered chains, T_θ is expected to be different than that of free chains. On the basis of what is known about branched polymers, we expect T_θ of our brush system to be lower (than 34.5 °C, which is T_θ for free PS chains in cyclohexane) due to additional repulsion arising from the tethered structure. As a result, the parameters K_π and ν need to be determined from experimental data. Rough estimates for ν and K_π can be obtained from the reduced force–distance data at high compression where the PTH model is valid. At high compression where osmotic forces dominate, the PTH model (eq 7) reduces to

$$F = XYd^{1/(3\nu-1)} \quad (11)$$

With a value of $\beta = 0.54$ calculated on the basis of the analysis presented in ref 30 and summarized in the Appendix, estimates for ν and K_π can be obtained from the slope and intercept, respectively, of the log F vs log d data at high compression: this yields $\nu = 0.5087$ and $K_\pi = 0.839$.

To further refine these estimates for ν and K_π , the PTH model can be recast in a form that will coalesce the universal profiles from different solvent conditions. This new scaling will superpose the master curves for brushes in good and near- Θ solvents that are shown in Figure 7:

$$F^* = 1 + d^* \quad (12)$$

where

$$F^* = \left(\frac{F}{X} + 1 + \frac{1}{4\nu - 1}\right) \left(\frac{4(3\nu - 1)K_\pi}{4\nu - 1}\right)^{-1/4\nu} \left(\frac{4\pi}{3\beta}\right)^{-(1-\nu)/2\nu(3\nu-1)} d^{1/(3\nu-1)} \quad (13)$$

and

$$d^* = \frac{1}{4\nu - 1} \left(\frac{4(3\nu - 1)K_\pi}{4\nu - 1}\right)^{-1} \left(\frac{4\pi}{3\beta}\right)^{2(\nu-1)/(3\nu-1)} d^{4\nu/(3\nu-1)} \quad (14)$$

To superpose the profiles for PS in toluene and in

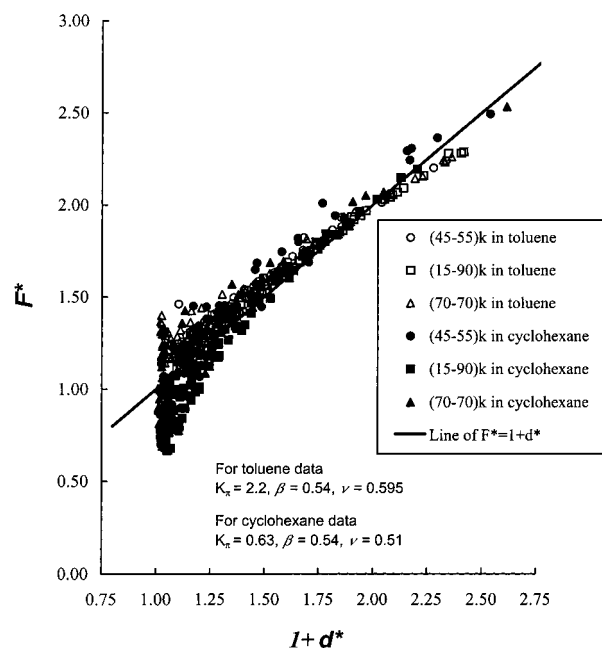


Figure 8. Reduced force–distance data for brushes formed from PVP–PS diblocks in toluene and cyclohexane created with the PTH model recast in a form that is independent of solvent quality. F^* and d^* were determined according to eqs 13 and 14, respectively. Coincidence of the PS/cyclohexane data with the profiles for the PS/toluene system is achieved with $\nu = 0.51$ and $K_\pi = 0.63$.

cyclohexane, the proper values of ν , K_π , and β must be used. To produce Figure 8, the values of ν and K_π for PS in cyclohexane were adjusted to obtain coincidence of the data. While the coincidence deduced from the universal profile is expected to be valid in general, the specific d^* dependence of F^* becomes invalid at weak compression where the assumptions used in producing the PTH model fail. As indicated by the legend in Figure 8, a value of $\nu = 0.51$ and $K_\pi = 0.63$ were found to produce the best superposition. This value K_π agrees with the data from Stepanek et al.,³⁹ and the expectation that K_π should have a value around unity at $c \sim c^*$ where the osmotic pressure makes a crossover from van't Hoff behavior to scaling behavior (cf. eq 3). The result that $\nu > 0.5$ is consistent with our assertion that cyclohexane is a marginal solvent for the tethered PS chains.

The values of ν and K_π obtained by superposing the data to produce Figure 8 were also used to create the PTH fit for PS in cyclohexane that is given by the solid line in Figure 7. As has been seen for brushes in good solvent,³ the reduced data are better fit at mid to high compression (small d) where the osmotic contribution is the more dominant contribution to the free energy of the layer. At low levels of compression, the PTH model appears to agree more closely with the PS/cyclohexane data than the PS/toluene system. This may reflect the fact that the segment density profile of the chains in the near- Θ solvent is more box-like than in good solvent; this was shown, for example, by molecular dynamics²¹ and Monte Carlo²⁰ simulations and neutron reflectivity experiments carried out by Levicky and co-workers.⁴² Although the data for brushes in cyclohexane in Figure 7 have been scaled with $\nu = 0.5$, this results in only a small shift of about 10% toward smaller F and d ; i.e., only 0.05 in the log–log scale. Thus, the data can be viewed as if $\nu = 0.51$ were used to scale the data that form this master curve in Figure 7.

The fact that the dimensionless universal profile expressed by eq 8 fits the PS/cyclohexane data is not surprising since the brushes exhibit analogous structural behavior in both solvents, as seen in Figures 2 and 3. Subtly this agreement between the data and model indicates that the physical assumption of noninterpenetration between opposing brushes is also fairly good for layers bathed in a near- Θ solvent. This buttresses the results of Hirz, who showed with SCF calculations that a brush in good and Θ solvents interpenetrate to similar degrees at similar levels of compression.¹⁶ As was seen from Figures 2 and 3, whether in cyclohexane or toluene, the forces of interaction between the brushes are repulsive, and the PS chains of the brush are stretched a few times their radius of gyration. The stretching dilutes the segment concentration and lowers the osmotic interactions. When opposing brushes are squeezed against one another, stretching to interpenetrate the other brush does not reduce the osmotic pressure, and therefore, the chains compress back along their contour length.

Conclusions

We have measured the forces of interaction between opposing brushes formed from PS–PVP block copolymers in good and near- Θ solvents and quantified changes that occur to the height of the layer when the solvent condition is changed. Our results are in accord with what is known about the structural behavior of brushes in a good solvent. In all cases, the forces between the brush layers are repulsive, and the chains are stretched a few times their free solution radii of gyration. The contraction of a monodisperse brush that occurs when the solvent is changed from toluene to near- Θ cyclohexane is significantly larger than the change in R_g of free coils under similar conditions and agrees with theoretical predictions and hydrodynamic measurements. We find that the structural changes in a brush made from a PS–PVP–PS triblock copolymer are controlled by the bimodal distribution of chains that comprise the layer.

Our results show that the force–distance data between the PS brushes bathed in each solvent can be coalesced to a unique master curve by the scaling suggested by a mean-field model. These universal curves, which scale the dependence on molecular weight and tethering density, can be predicted by the PTH model with the aid of three constants: ν , K_π , and β . In each solvent, the value of β is determined by comparing the osmotic free energy of tethered chains to free coils. For brushes in the good solvent (toluene) the PTH model agrees with the reduced SFA data using values of ν and K_π obtained from measurements on bulk solutions. Data from bulk solutions cannot be used, however, to produce agreement between the PTH model and experimental data from the PS/cyclohexane system near the (bulk) Θ temperature. An additional repulsion arising from the tethered structure suppresses the Θ temperature, making cyclohexane at 32 °C a marginal solvent for PS brushes. (This effect on T_θ is similar to what occurs with branched chains in solution.) The extra monomer–monomer repulsion was evidenced by comparing the osmotic contribution to the free energy of the brush to that of a homopolymer solution of the same average concentration. By recasting the PTH model in a form that scales the dependence on solvent quality, we find that the reduced force–distance data for brushes in

cyclohexane superpose with the data from toluene when $\nu = 0.51$.

The agreement between the reduced force–distance data and the PTH model confirms that the assumptions used in the mean-field picture also apply to brushes in a near- Θ solvent. Notably, the mean-field model assumes that there is minimal interpenetration between opposing brushes: when brought into compression, chains from opposing brushes collapse back along their contour length rather than interpenetrate. The fact that brush covered surfaces behave similarly under compression in both good and near- Θ solvents will be generally useful for devising avenues for tailoring interactions between surfaces. The results form a more complete picture of the structural behavior of brush systems.

Acknowledgment. We acknowledge support for this work from several sources: Funding from the Center for Interfacial Engineering, an NSF funded ERC at the University of Minnesota, the Interfacial Transport and Separations Program of the NSF (S.M.K.II: NSF-CTS-9816147; M.T.: NSF-CTS-9616797), and the Petroleum Research Fund, administered by the American Chemical Society (Grant 32514-G7), is gratefully acknowledged. H.W. acknowledges, with thanks, support from Japan Chemical Innovation Institute (through the Doi Project for development of Platform for designing high functional materials).

Appendix

Recently, we presented³¹ an analysis showing how the distinct chain conformations adopted by brushes and by coils in free solution lead to differences in the correlation length of tethered chains and untethered chains in semidilute solution (at the same concentration). Here we summarize the salient features. As discussed in refs 3 and 31 and in this paper, specifically with regard to Figure 5, the osmotic contribution to the free energy of the brush will be underestimated if the correlation length for coils in free solution, ξ_s , is used:

$$\xi_s = R_g \left(\frac{c}{c^*} \right)^{-\nu/(3\nu-1)} = \left(\frac{3m_0}{4\pi N_{Av}} \right)^{\nu/(3\nu-1)} b^{-1/(3\nu-1)} c^{-\nu/(3\nu-1)} \quad (A1)$$

Using this expression to derive the osmotic free energy as a function of concentration for a brush that obeys the Alexander–de Gennes ansatz yields

$$f_{os,s}(c) = (3\nu - 1)kTQ_s' \left(\frac{m_0}{N_{Av}} \right)^{-3\nu/(3\nu-1)} a^{3/(3\nu-1)} w c^{1/(3\nu-1)} \quad (A2)$$

with

$$Q_s' = K_\pi \left(\frac{2^{1/2}\pi}{3^{5/2}} \right)^{1/(3\nu-1)} \quad (A3)$$

In these expressions, $a \cong \sqrt{6}b$ and other variables have the same definitions as in the text of this paper. As shown by Watanabe and Tirrell, in toluene there was roughly a factor of 2 difference between the osmotic free energy of the brush determined from SFA experiments (i.e., eq 1) and $f_{os,s}$.³ Agreement could be achieved by replacing when c^* with βc^* (in eq A1), where $\beta' = \beta^{-1/(3\nu-1)} \cong 2$. However, reformulating the PTH model

on the basis of a new correlation length for the tethered chains, ξ_b , brings the model into agreement with the experimental data.

$$\xi_b = BQ_b^{\nu/(3\nu-1)} \left(\frac{m_0}{N_{Av}} \right)^{\nu/(3\nu-1)} a^{-1/(3\nu-1)} c^{-\nu/(3\nu-1)} \quad (A4)$$

In this expression, the numerical factors Q_b and B are given by

$$Q_b = \frac{2^{(\nu-1)/\nu} (3\nu - 1) K_\pi}{\pi (4\nu - 1) B^{(1+\nu)/\nu}} \quad (A5)$$

and

$$B = \left[\frac{3(3\nu - 1) K_\pi}{2\pi^2 (4\nu - 1)} \right]^{1/4} \quad (A6)$$

Using the correlation length ξ_b to derive the osmotic free energy of a brush as a function of concentration results in the following expression:

$$f_{os,b}(c) = (3\nu - 1)kTQ_b' \left(\frac{m_0}{N_{Av}} \right)^{-3\nu/(3\nu-1)} a^{3/(3\nu-1)} w c^{1/(3\nu-1)} \quad (A7)$$

where

$$Q_b' = K_\pi \left(\frac{\pi}{6} \right)^{1/(3\nu-1)} \quad (A8)$$

It should be noted that eqs A7 and A2 have the same concentration dependence, but their magnitudes are different:

$$\begin{aligned} \frac{f_{os,b}(c)}{f_{os,s}(c)} &= 2.17 \quad (\text{for } \nu = 0.595) \\ &= 3.375 \quad (\text{for } \nu = 0.5) \end{aligned} \quad (A9)$$

Thus, the osmotic free energy of the brush determined by using a correlation length based on a homogeneous uncompressed brush is greater than the osmotic free energy of the brush formulated on free coils in solution (and β can be calculated from this ratio).

An explicit expression for the equilibrium height of the brush, L_{eq} , was found by minimizing the total free energy of the brush (which includes the osmotic swelling and elastic stretching contributions to the free energy), which had been formulated on the basis of eq A4:

$$L_{eq} = Q_b a^{1/\nu} \sigma^{(\nu-1)/2\nu} N \quad (A10)$$

Combining this expression with eqs A5 and A6 and proper parameters for PS in toluene and cyclohexane (at 32 °C) yields the L_{ToI}/L_{CH} results given in the rightmost column of Table 3.

References and Notes

- (1) Hadziioannou, G.; Patel, S.; Tirrell, M. *J. Am. Chem. Soc.* **1986**, *108*, 2869–2876.
- (2) Tirrell, M.; Patel, S.; Hadziioannou, G. *Proc. Natl. Acad. Sci. U.S.A.* **1987**, *84*, 4725–4728.
- (3) Watanabe, H.; Tirrell, M. *Macromolecules* **1993**, *26*, 6455–6466.
- (4) Dhoot, S.; Watanabe, H.; Tirrell, M. *Colloids Surf. A* **1994**, *86*, 47–60.

- (5) Patel, S. S.; Tirrell, M. *Annu. Rev. Phys. Chem.* **1989**, *40*, 597–635.
- (6) Webber, R. M.; van der Linden, C. C.; Anderson, J. L. *Langmuir* **1996**, *12*, 1040–1046.
- (7) Granick, S.; Demirel, A. L.; Cai, L. L.; Peanasky, J. *Isr. J. Chem.* **1995**, *35*, 75–84.
- (8) Karim, A.; Satija, S. K.; Douglas, J. F.; Anker, J. F.; Fetters, L. J. *Phys. Rev. Lett.* **1994**, *73*, 3407–3410.
- (9) Klein, J.; Perahia, D.; Warburg, S. *Nature* **1991**, *352*, 143–145.
- (10) Prucker, O.; R  he, J. *Macromolecules* **1998**, *31*, 592–601.
- (11) Prucker, O.; R  he, J. *Langmuir* **1998**, *14*, 6893–6898.
- (12) Alexander, S. J. *Phys. (Paris)* **1977**, *38*, 983–987.
- (13) de Gennes, P. G. *Macromolecules* **1980**, *13*, 1069–1075.
- (14) Milner, S. T.; Witten, T. A.; Cates, M. E. *Macromolecules* **1988**, *21*, 2610–2619.
- (15) Milner, S. T. *Europhys. Lett.* **1988**, *7*, 695–699.
- (16) Hirz, S. J. Masters Thesis, University of Minnesota, 1986.
- (17) Cosgrove, T.; Heath, T.; van Lent, B.; Leermakers, F.; Scheutjens, J. *Macromolecules* **1987**, *20*, 1692–1696.
- (18) Dolan, A. K.; Edwards, S. F. *Proc. R. Soc. London A* **1975**, *343*, 427–442.
- (19) Milner, S. T. *J. Chem. Soc., Faraday Trans.* **1990**, *86*, 1349–1353.
- (20) Lai, P. Y.; Binder, K. *J. Chem. Phys.* **1992**, *97*, 586–595.
- (21) Grest, G. S.; Murat, M. *Macromolecules* **1993**, *26*, 3108–3117.
- (22) Auroy, P.; Mir, Y.; Auvray, L. *Phys. Rev. Lett.* **1992**, *69*, 93–95.
- (23) Mansfield, T. L.; Iyengar, D. R.; Beaucage, G.; McCarthy, T. J.; Stein, R. S.; Composto, R. J. *Macromolecules* **1995**, *28*, 492–499.
- (24) (a) Koningsveld, R.; Kleintjens, L. A.; Shultz, A. R. *J. Polym. Sci., Part A-2* **1970**, *8*, 1261–1278. (b) Derham, K. W.; Goldsbrough, J.; Gordon, M. *Pure Appl. Chem.* **1974**, *38*, 97–116.
- (25) Kilbey, S. M., II.; Schorr, P.; Tirrell, M. In *Dynamics of Small Confining Systems IV*; Drake, J. M., Grest, G. S., Klafter, J., Kopelman, R., Eds.; Materials Research Society: Pittsburgh, PA, 1999.
- (26) Appelt, B.; Meyerhoff, G. *Macromolecules* **1980**, *13*, 657–662.
- (27) Kniewske, R.; Kulicke, W. M. *Makromol. Chem.* **1983**, *184*, 2173–2186.
- (28) Nakamura, Y.; Norisuye, T.; Teramoto, A. *Macromolecules* **1991**, *24*, 4904–4908.
- (29) Derjaguin, B. V. *Kolloid Z.* **1934**, *69*, 155–164.
- (30) Dan, N.; Tirrell, M. *Macromolecules* **1993**, *26*, 6467–6473.
- (31) Watanabe, H.; Kilbey II, S. M.; Tirrell, M. *Macromolecules* **2000**, *33*, 9146–9151.
- (32) Kelley, T. W.; Schorr, P. A.; Johnson, K. D.; Tirrell, M.; Frisbie, C. D. *Macromolecules* **1998**, *31*, 4297–4300.
- (33) Halperin, A. *J. Phys. (Paris)* **1988**, *49*, 547–550.
- (34) Parsonage, E.; Tirrell, M.; Watanabe, H.; Nuzzo, R. G. *Macromolecules* **1991**, *24*, 1987–1995.
- (35) Miyaki, Y.; Einaga, Y.; Fujita, H. *Macromolecules* **1978**, *11*, 1180–1186.
- (36) de Gennes, P. G. *Scaling Concepts in Polymer Physics*; Cornell University Press: Ithaca, NY, 1979.
- (37) des Cloizeaux, J.; Noda, I. *Macromolecules* **1982**, *15*, 1505–1507.
- (38) Noda, I.; Higo, Y.; Ueno, N.; Fujimoto, T. *Macromolecules* **1984**, *17*, 1055–1059.
- (39) Stepanek, P.; Perzynski, R.; Delsanti, M.; Adam, M. *Macromolecules* **1984**, *17*, 2340–2343.
- (40) (a) Candau, F.; Strazielle, C.; Benoit, H. *Makromol. Chem.* **1973**, *170*, 165–176. (b) Roovers, J. *Polymer* **1979**, *20*, 843–849. (c) Decker, D. *Makromol. Chem.* **1969**, *125*, 136–160.
- (41) Higo, Y.; Ueno, N.; Noda, I. *Polym. J.* **1983**, *15*, 367–375.
- (42) Levicky, R.; Koneripali, N.; Tirrell, M. *Macromolecules* **1998**, *31*, 3731–3733.

MA001343K